

S-TFRC: An Efficient Rate Control Scheme for Multimedia Handovers

Imdad Ullah*, Zawar Shah[‡], and Adeel Baig*

*The University of New South Wales (UNSW), Sydney, Australia.

[‡]Whitireia Community Polytechnic, Auckland, New Zealand.

*College of Computer and Information Systems, Al Yamamah University, Saudi Arabia.

*School of Electrical Engineering & Computer Science (SEECS), National University of Sciences & Technology (NUST), Islamabad, Pakistan.

email: imdadu@cse.unsw.edu.au; zawar.shah@whitireia.ac.nz; adeel.baig@seecs.edu.pk

Abstract. The integration of heterogeneous wireless access technologies has numerous issues for multimedia applications, such as to smoothly continue over new connections without any service disruption during vertical handovers. We propose State-Aware Feedback extension to Datagram Congestion Control Protocol (DCCP) that meets QoS requirements of multimedia applications throughout the handover process. We consider movement of mobile subscribers among heterogeneous access technologies from highly unstable to more stable environment and model their mobility patterns as Uniform, Pareto, and Exponentially distributed. We present detailed analysis on the performance of proposed mechanism in terms of resuming transmissions during the handover process. In particular, we propose Markov model of TFRC capturing TCP timeouts, loss rates, and no-feedback timer expirations. We validate the proposed analytical model through simulations and show that it accurately predicts various congestion events that may happen during the handover process. We then evaluate the performance of S-TFRC via both simulations and analytical model and observe the sender rates and throughputs achieved. We also consider transmission delays and transmission rates as performance metrics and compare performance of S-TFRC with the standard TFRC. Our results show that S-TFRC is capable of providing better QoS to multimedia applications than standard TFRC by significantly reducing transmission delays and provides better throughput to multimedia applications.

Keywords: vertical handover, link stability, heterogeneous networks, DCCP, TFRC, S-TFRC, WiMAX, LTE.

1. Introduction

As the internet grows, the mobile broadband service provisioning is becoming a reality and it is probable that about 3.4 billion subscribers will have broadband internet access in the next couple of years and majority of these subscribers will be served up by wireless broadband technologies [1]. To ensure end-to-end connectivity and guaranteed Quality of Service (QoS) requirements for multimedia applications; several proposals have been suggested by IETF such as DCCP at the transport layer [2]. Similarly, the emergence of new concepts like seamless connectivity to high performance services and serving multimedia applications anytime and anywhere, irrespective of users' locations, has led to the integration of third and fourth generation networks. As an example, the integration of Worldwide

Interpretability for Microwave Access (WiMAX) and Long Term Evolution (LTE) to the legacy wireless local area networks based on IEEE 802.11 standards using dual-mode operations [3]. To allow the subscriber devices opt interchangeably between such heterogeneous networks; many vertical handover strategies have been suggested [4][5][6].

Multimedia applications, such as VoIP, video conferencing etc. running over mobile devices are disrupted because of the different characteristics of heterogeneous wireless technologies [7][8]. The transport layer that ensures end-to-end connectivity [7] requires that the connection endpoints must adapt their transfer rates according to the link characteristics [6]. For example, transport mechanisms manage transmission rates by collecting information such as Round-Trip Time (RTT), packets received rate and the loss event rate from the network. However, during the handover process, a sudden change in the link attributes makes the environment un-related and it becomes hard for these mechanisms to determine state of the network [8]. This causes disruption to multimedia sessions. The situation becomes worse when frequent handovers among different access technologies occur [5][9].

In this paper we propose State Aware DCCP that is a feedback scheme, which gathers state of the networks during the handover process. It is implemented via explicit handover notifications and exchange of link parameters via link characteristics information (LCI) option present in Mobile IP (MIP) [10]. The exchange of link parameters according to the type of access technology is already proposed in [10]. However for S-DCCP, we suggest to pass more specific parameters to determine various link parameters and timely negotiate the transmission. To begin with, one of the important parameters is the link utilization i.e. how many packets are successfully served by the intermediate routers and end nodes under the State Aware scheme, which is termed as S-utilization. Another important parameter is the State Aware RTT (S-RTT) that helps respective nodes to calculate link congestion states and the link's contexts such as the wireless access type, delay and bandwidth etc. Finally, we propose a mechanism to detect change in wireless access network of the correspondent nodes (CNs) to trigger the handover process.

Based on these parameters, the mobile node (MN) approve new rate request from intermediate access routers and the CNs. The MN then adjust new rate according to the link characteristics (such as available bandwidth etc.) of the newly visited network. The exchange of these parameters help in efficient utilization of the networks whether the handover occurs from low-bandwidth to high-bandwidth provisioning networks or vice versa. Such an example when a MN handovers from GPRS to WiMAX or from WiMAX to GPRS. Although sufficient bandwidth is available but default mechanisms fail to realize it and continue over low rates until the transport layer mechanism slowly probes the new network over several RTTs [11]. We evaluate the scheme for various mobility scenarios, such as the MNs moving with vehicular speeds to nomadically roaming among different wireless technologies. We further evaluate the disruptions and performance degradations against link stability that is characterized by the frequency and distribution of handovers. For instance, the MNs having handovers after every 10sec is highly unstable compared to the one that makes handovers with every 100sec of intervals. The scheme holds for both variants of DCCP i.e. TCP-Like and TCP Friendly Rate Control (TFRC) and the new mechanisms under the S-DCCP are termed as S-TCPLike and S-TFRC respectively. We argue that the proposed mechanism does not require major changes to the existing working mechanism of DCCP and can be implemented in real-world environment with less

overheads. The mobile subscribers would also appreciate achieving better performance of communicating multimedia applications while they move around with different speeds of roaming and while connecting/disconnecting to different access technologies.

We further develop an analytical model that captures different states of TFRC and S-TFRC during vertical handovers in terms of loss event rates, effect of timeouts, feedback timer expirations, and average round trip times. The proposed analytical model is additionally evaluated for the probabilities during congestion events such as timeouts, duplicate acknowledgements etc. The model also provides an estimate of the throughput and sending rate that are achieved by MNs with various mobility patterns and link stabilities. We note that this modeling has not been considered that captures different events of congestion control behaviors associated with the MNs during the vertical handover processes.

Our main contributions in this work are (i) To develop State Aware mechanism that meets QoS constraints for media transport during vertical handovers. (ii) To propose a Markov model that depicts TFRC and S-TFRC behaviors in terms of loss event rates, effect of timeout and no-feedback timer expirations. The model is also validated via simulations. (iii) To determine the impact of vertical handovers on the performance of real time multimedia applications using S-TFRC. (iv) To quantify the improvement in throughput and transmission rates provided by S-TFRC compared to the standard TFRC via analytical model and simulations. (v) To calculate the transmission delays and loss behaviors of standard TFRC and S-TFRC in different handover scenarios via simulations.

The rest of the paper is organized as follows. Section 2 provides necessary background on the congestion control mechanisms of DCCP along with the motivation for its use in vertical handovers. Section 3 gives an overview of related work on transport mechanisms during vertical handover. It further provides comparison of the proposed work with the state of the art works in vertical handovers. Section 4 formulates the problem. Section 5 presents the proposed scheme describing the simulation environment and the simulation model. Section 6 presents the analytical model for calculating different probabilities of congestion events during the handover process. Section 7 provides the validation of the proposed analytical model. Section 8 provides results and performance comparisons of TFRC with S-TFRC via analytical model and simulations. Finally, the conclusion is drawn in Section 9.

2. Background

For better media transport and due to growth of multimedia applications over the Internet, such as VoIP and video conferencing etc., the Datagram Congestion Control Protocol (DCCP) [13] has been proposed by Internet Engineering Task Force (IETF). DCCP is a good candidate intended for a replacement protocol for UDP in real-time multimedia applications. DCCP provides congestion-controlled transport layer transmission like TCP with reliable connection establishment/termination but unreliable data transmission like UDP. It provides two congestion control mechanisms, namely the TCP Friendly Rate Control (TFRC) [2] (Congestion Control ID 3 (CCID-3)) [12] and the TCP-Like also identified as Congestion Control ID 2 (CCID-2). TFRC is a rate-based congestion control mechanism [12], which provides a TCP-friendly rate by minimizing abrupt rate changes as in TCP so that data is sent smoothly during the whole voice communication. This

feature for transport of multimedia applications is important during when handovers occur, especially when mobile users experience frequent handovers. On the other hand, the abrupt changes in sending data rate (as with the TCP-Like) slows down the sending rate [2] thus the packets have to wait in sender's queue for some amount of time to be served to the destination. The congestion control mechanisms can be negotiated between the two communicating parties through the feature negotiation [13] at the connection setup or during communication.

Another important feature that DCCP provides is the Late Data Choice [14] where DCCP can adapt to constantly changing network conditions. This feature is important for multimedia applications that can adapt different kind of delays [15][16], which a particular data packet can experiment. Hence the mobile users can benefit when there are vertical handovers among the low and high bandwidth provisioning access technologies, such as handovers between GPRS and LTE. We achieved enhanced performance in transporting multimedia applications during the handover processes by modifying the basic mechanism of DCCP's exchange of different parameters (i.e. S-DCCP described in detail in Section 5) along with the use of DCCP-Quick Start (QS) [31].

3. Related Work

Recent improvements for vertical handover process suggest selection of appropriate access technology between WiFi and WiMAX based on analytical hierarchical process [17], an architecture based on MIH signalling for handover process between WiFi and LTE-Advanced [18], an architecture of network mobility (NEMO) in satellite link based on sensing information [19], and a game-theoretic model for selecting suitable access network by capturing inter-linkages of various networks [20]. In a highway with vehicles moving at high speeds in different directions, the authors [21] suggest pre-handover procedure to maintain internet connectivity, using vehicular ad hoc networks (VANETs). The link information is acquired from the vehicles using multi-hop relays that are moving in either directions and thus reducing the handover delays. The authors in [22] propose a Call Admission Control (CAC) strategy using adaptive multiguard channel scheme for prioritizing traffic types and handover calls while guaranteeing the fulfilment of QoS requirements. Similarly, [23] proposes a scheme based on identifier-to-locator mappings of mobile nodes, which helps reducing the connectivity disruption and also enhances reliability for managing their locations.

Comparison with other works: In [24], the authors propose a distributed vertical handover decision making scheme that is integrated with IEEE802.21 Media Independent Handover (MIH) to enhance the handover decision by communicating messages provided by MIH Function (MIHF) among the mobile nodes and the access technologies. However, this solution does not provide unique network characteristics among the various access technologies that make it hard to calculate the quality of the available networks and hence to increase the performance evaluation needed. In [25], the authors propose a handover scheme using the Simple Additive Weighting (SAW) and the Weighted Product Model (WPM) methods to select the best network among the available heterogeneous access technologies. This scheme reduces the handover processing delays. Another work [26] compares the SAW and the Technique of Order Preference by Similarity to Ideal Solution (TOPSIS) to find best selection method in order to reduce the processing delay

during the handover process. Similarly, the [27] and [29] respectively use the TOPSIS and Grey Relation Analysis (GRA) methods to choose the best available networks and reduce the handover delays. However, all these schemes do not provide any specific method for generating the weight parameters that are used under the SAW, TOPSIS, and GRA methods.

Furthermore, the [28] analyzes and validates the TOPSIS algorithm under various handover scenarios with different QoS requirements. Nevertheless, this scheme has high level of complexity of implementation due to the integration of many networks' parameters. The [30] proposes a four-step integrated method for Multiple Attribute Decision Making (MADM) based method to solve the network selection issues. The authors identify important network selection issues such as the usage of handover properties, the requirements of efficient weighting method, and the trade-off for handovers to the new best network. However, this study does not provide the techniques for solving these network selection issues within the scope of MADM-based network selection process. In our work, we have proposed and validated by implementing a feedback scheme that gathers context of handovers and link information during the network selection process. This timely negotiates the transport mechanisms of both the sender and the receiver. We further have proposed a Markov model that identifies various congestion events of timeouts, loss rates, and no-feedback timer expirations that may happen during the vertical handover processes and could disturb the on-going multimedia transport sessions.

Our work find its inspiration from IETF's DCCP-Quick Start (QS) [31] and the proposal of delivering the access link characteristic information using MIP signaling [10]. QS is an experimental extension proposed first for TCP [11] that side-steps the time-consuming network probing by Slow-Start and allows hosts to request for a higher sending rate by explicitly asking permissions from the network nodes such as routers and end hosts. TCP-QS extension has shown significant performance improvement for best effort data transport in terms of transfer time of data and throughput achieved over satellite, GPRS and Wi-Fi networks [11][32]. However, performance evaluation for DCCP-QS in vertical handovers has not been studied in the existing literature. Also, to the QS, there are some open questions [11] like when a node should initiate QS and determine QS rate to request for. A decision on these parameters is challenging when a node is mobile and undergoes vertical handover(s) because the new access characteristics are not related to previous environment. Considering these challenges, a mechanism that satisfies QoS for multimedia in vertical handovers is needed. Our idea is to provide an informed mechanism that not only rectifies the concerns of QS but also distinguishes itself in terms of improved network utilization for media transport. It timely notifies the respective nodes about the link changes and triggers State Aware feedbacks to adjust transport accordingly.

4. Problem Formulation

For media transport over homogenous wired networks, various transport protocols exist such as UDP, DCCP variants TCPLike and TFRC etc. However, with the emergence of future wireless heterogeneous systems, where mobile subscribers share several network resources, require flow control and congestion control mechanisms to ensure seamless connectivity. The widely used UDP does not support the QoS constraints for media appli-

cations [8]. Similarly DCCP's behavior in heterogeneous wireless networks needs extensive improvements to address issues during the handover process [7][3][33].

We formulate a study on one of such connectivity problems regarding the performance degradations to wireless clients' sessions in various mobility scenarios. We perform the vertical handover between a cellular network (i.e. GPRS) and the broadband access technologies i.e. WiMAX and LTE. Assuming a MN connected to GPRS experiences varied signal strength. Since near the Base Stations (BS) the signal strength is relatively high compared to the far coverage areas. As a result, the MN observes a disruption perhaps a disconnect, a re-selection and then finally session resumes. Hence, the MN performs handovers between the two types of wireless access technologies. We simulate the vertical handover environment as shown in Figure 1 and use the same simulation parameters as given in Table 1. We further take various link stabilities of 10s and 100s and various handover distributions of Uniformly (U), Pareto (P), and Exponential (E). Detailed descriptions of handover distributions and the simulation modeling/environment are given in Section 5.

Table 1. Simulation Parameters

Parameters	Values
Traffic	CBR (real time) size: 512bytes rate: 10ms
Wired	Bandwidth: 100Mbps Delay: 15ms
Data rate	155.2Kbps - 74Mbps (GPRS-WiMAX)
Latency	15ms - 20ms
Bandwidth	5MHz - 20MHz
Subcarrier Spacing	10KHz - 15KHz
Frame Duration	5ms - 240ms
Symbol/Preamble Duration	16microsecond - 16ms

Figure 2 demonstrates transmission delay and throughput with various handover distributions and multimedia applications running over UDP and DCCP variants i.e. TCP-Like and TFRC. To the right of the figure the link stability increases and handover frequency decreases. The results verify that during handover, UDP having no flow control acts with its statelessness, fails to gather link states for several seconds. As an example, with link stability of 10 it takes 0.65s for clients to resume transmission (shown as 'dotted line with circles' in Figure 2(a)). This situation worsens with increase in handover frequencies and link losses as a transmission loss of 75% is observed for U-UDP. The packet loss worsens for E-UDP (84%) and for P-UDP (95%) (due to space limit the results for link losses are not presented). On the other hand, for the same link stability of 10, U-TFRC provides an average delay of 0.35s while this value worsens to 0.85s with increased losses. Similar observations is also found for throughput as shown in Figure 2(b). At the link stability of 50s, UDP achieves a low throughput of 0.06Mbps. However with the same link stability of 50s, U-TFRC manages 6.4Mbps while U-TCPLike provides 0.43Mbps throughput for multimedia applications' transport. Moreover, it can be seen that handover distributions greatly affect the delay and throughput observed for various transport mechanisms. It can be analyzed that for U and E-handovers, the corresponding system becomes aware of the environment and the MNs understand the frequency and

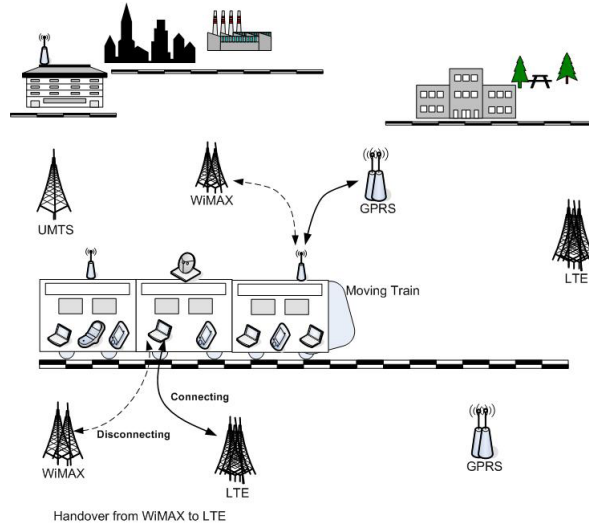


Fig. 1. Vertical Handover Scenario.

possible occurrences of handovers, therefore adjusts after sometime. On the other hand, a continuous degradations in the P-handovers are observed due to the congestion of the nodes connected to different access technologies. Hence, it follows that present transport mechanisms fail to meet the QoS constraints for transporting multimedia applications during the vertical handover processes.

To overcome this, we propose S-DCCP Feedback - a vertical handover enhancement for transporting multimedia applications where the mechanism allows timely negotiation of transport mechanisms for the end clients during handover such and quickly recovers the on-going sessions.

5. Proposed Scheme

In this section, we present the proposed S-DCCP Feedback mechanism with the method for exchanging State-Aware parameters to smoothly continue over new connections and setting of new transmission parameters. We first discuss the vertical handover environment and then present detailed description of simulation model. The analytical model is presented in the next section.

5.1. Vertical Handover Environment

In the proposed scheme we exploit the loose coupling architecture where for example, the WLAN network would act as an access network and would not be connected directly to the core GPRS/UMTS network. The scenario of interest is simulated as in Figure 1. The arrows show the subscriber's route and possibility of a typical vertical handover comprising of a WLAN (IEEE 802.11b/g), cellular network (GPRS) and broadband access

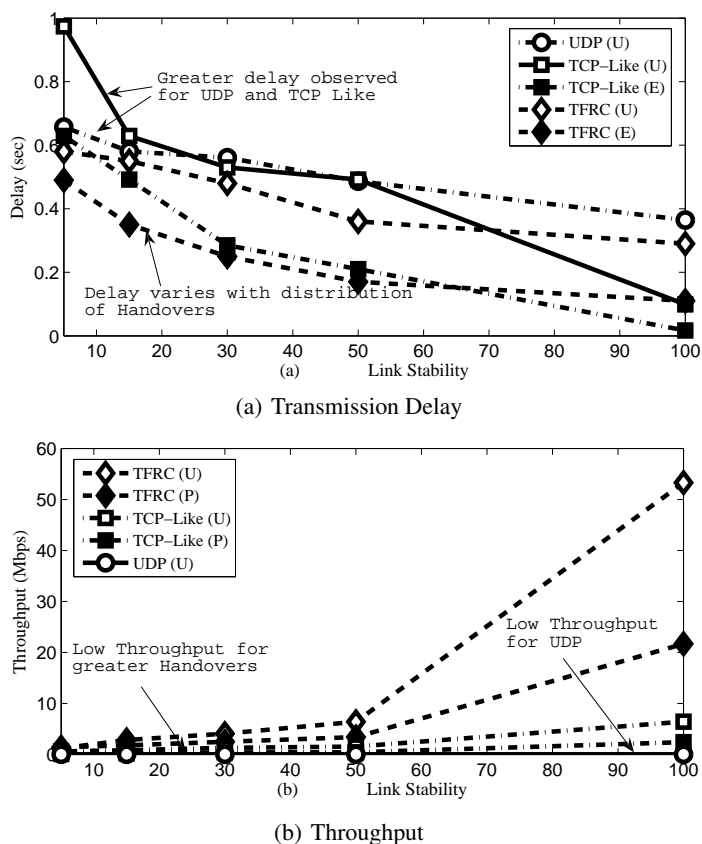


Fig. 2. Transmission Delay and Throughput during Vertical Handover.

networks i.e. WiMAX and LTE. The various simulation parameters are given in Table 1. Note that the term multimedia applications (and hence the multimedia handovers) is specifically used for real-time applications such as VoIP, video conferencing etc.

The considered simulation environment is taken as follows: an MN connected via GPRS sets out on a journey that includes the route via non-congested areas such as a highway and some part of travel from congested regions, such as the city center. To reflect these handovers, we consider the MN as moving with uniform speed and thus is simulated as Uniformly distributed (U). Similarly, for the congested regions the handovers are modeled with Pareto distribution (P) while handovers for the entire journey i.e. both congested and non-congested areas are considered to be Exponentially distributed (E). These usage models are in line with the practical network models discussed in [34]. Furthermore, in our scenario, we assume that the MN remains connected to GPRS network for most part of its travel (since GPRS is almost ubiquitous [35]). The MN handovers only at regions where signal strength drops near the edges of GPRS coverage or strong signals from other access coverages are observed. We further take the scenario where the

new connection is established before the connection to the older access network is broken [4] during the handover process. Error losses over links are respectively kept as low, medium, and high to demonstrate the performance degradations to multimedia sessions in a real wireless heterogenous network. The MN is designated as the S-TFRC receiver, while another node called the correspondent node (CN) acts as the S-TFRC sender and is located at the back of the broadband network. All the traffic from CN is routed through the MN's Home Agent (HA).

5.2. Simulation Model

For the performance evaluation of S-DCCP during vertical handovers we used Network Simulator NS-2.34. Default NS-2 only has 802.11b implementation. We had to incorporate DCCP module and support for 802.11g, GPRS, WiMAX and LTE technologies based on IEEE standards. This is achieved by modifying the MAC and PHY layers' parameters as illustrated in Table 1. We kept the size of bottleneck link, taken as the lastmile i.e. between FA to the MN, to minimum to prevent data loss during handover process. Next, we implemented modules for S-DCCP including S-Feedback Request, S-Feedback Response, and S-Feedback Process that generate S-Feedback options for determine transmission parameters after handover. S-Feedback options and handover notifications are exchanged between nodes by exploiting either the data packets (DATA-ACK) or the acknowledgement (ACK) packets without putting any burden over the network. Our modifications do not require any extra protocol changes than defined for LCI option for Mobile IP and DCCP-QS proposals assuming that the intermediate nodes support these.

Figure 3 shows the S-Feedback option in the IP header of DATA-ACK or ACK. S-Feedbacks are defined via type field that states whether an S-Request, S-Response or an S-Process option is being sent. The length field specifies S-Option length and is set to 8 bytes [31]. $S - TTL$ specifies an arbitrary Time-To-Live (TTL) value. The rate field determines the requested/approved S-Rate in bytes per second and $Diff - TTL$ stores the difference between $IP - TTL$ and $S - TTL$ that verifies if S-Requests and S-Responses are valid. These S-Feedback options are generated via modules running at the sender's and receiver's S-DCCP layers. These modules gather handover context along with the link characteristics, determine transmission parameters for the end nodes, and timely negotiate in handover process. Their implementations are as under.

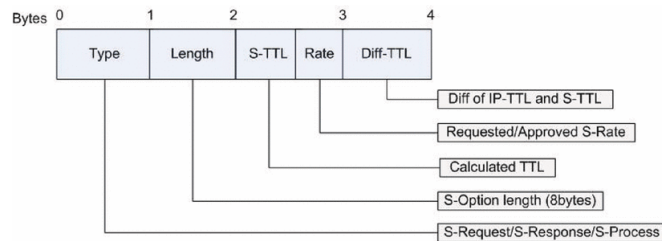


Fig. 3. State Aware Feedback Option.

- **S-Feedback Request** module determines, when a sender triggers S-Request i.e. at the start of handover, the number of S-Requests made and sets a back-off interval; the time during which new S-Requests cannot be made. S-DCCP sender on receipt of handover flag and link characteristics information makes S-Request by specifying the desired initial S-Rate and an arbitrary $S - TTL$. In order to ensure that unnecessary S-Requests are not generated, the back-off interval is calculated as: $back - offInterval = \max(back - offInterval * 2, 4 * RTT)$ [31]. The unnecessary S-Requests can be generated due to congestion events or network delays, such as when packets carrying handover or link information reaches late for the same handover event. If back-off Interval exceeds a threshold then it forces the sender to revert to the default DCCP flow control.
- **S-Feedback Response** module runs at every router along the path and the receiver to process the S-Rate received in S-Request option. If the network routers' downstream link utility is low then the S-Rate is approved by decrementing both the $S - TTL$ and $IP - TTL$ by 1. Otherwise these parameters are set to zero if either a lower S-Rate is filled or they do not approve S-Rate. At the receiver, if S-Rate is permissible, the S-Response option is prepared by setting the rate field to the S-Rate and the $Diff - TTL$ field is filled with the difference of the received $IP - TTL$ and the $S - TTL$.
- **S-Feedback Process** module at S-DCCP sender computes the difference between the $S - TTL$ and the $IP - TTL$ on reception of the S-Response option. This difference is then passed along with the current S-Rate as the S-P type response to the S-DCCP receiver. The receiver validates these values and sends the S-P response option back to the S-DCCP sender. It checks the validity of the response by examining the $Diff - TTL$ and the rate fields. If it is valid then the sender computes its S-Window (S_{wnd}). Assuming S_{wnd} be greater than the C_{wnd} value, the corresponding hosts then increase their transmissions by S_{wnd} and after single RTT of successful S-Mode returns to their basic flow control. The RTT in this case is determined by ACK received of any of the data packets that was sent under State Aware.

Now we detail the how corresponding nodes determine access change and triggers S-DCCP to calculate the transmission parameters. At the time of handover, the handover notification flags over DATA-ACK or ACK and link parameters in mobile IP binding are explicitly passed to the CN's S-DCCP layer. This potentially identifies handover occurrence and link context i.e access type, delay, bandwidth and S-Parameters, as shown in Figure 4. At the same time, respective nodes store the present transmission state i.e. present window, present congestion window (S_{wnd}) and ACK. With this and the newly roamed network's information, the sender makes an informed decision on available BW calculated as $(link\ BW - link\ utilization - pending\ S - Requests)$, which is used to find required S-Rate as $present\ window * available\ BW$. This rate is used by CN to trigger S-Feedback request module to send S-Request to other nodes along the path. The S-Feedback response module then generates S-Response once the network routers and receiver accept the S-Rate (since the sender makes an informed decision on the rate request). Finally S-Feedback process module stimulates CN to start transmission with the approved S-Rate by calculating S_{wnd} as $(S - Rate * RTT / MSS)$, where RTT is the measured path round-trip delay and MSS is the maximum segment size in bytes. Besides, it also adjusts the TFRC receiver Feedback reports instead of receiver state i.e. according to the new available bandwidth after handover.

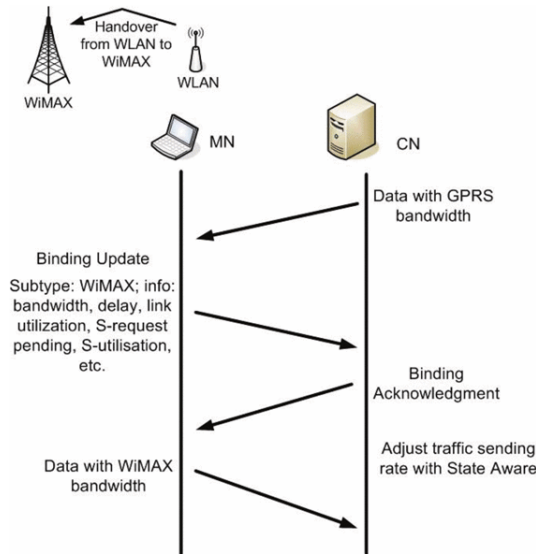


Fig. 4. Parameters in Proposed Link Characteristic Information.

6. Analytical Model

The motivation behind this analytical modelling is to evaluate the achieved enhanced performance of TFRC using proposed QS implementation for DCCP-TFRC for various congestion events during the vertical handover process. This model is based on the DCCP-QS for TFRC [31], which avoids prolonged network probing by slow-start and allows path nodes to agree on a higher sending rate by explicitly approving rate requests from all the nodes, along with providing access link information by means of MIP signalling [10].

This model also evaluates the probabilities that the mobile subscribers remain within a congestion event while roaming from one access technology to another. These events are the TFRC congestion control behaviour in different scenarios of timeout, duplicate acknowledgements, and the process of feedback packet's expiration and its reception at the sender TFRC. The sender rate is calculated by means of the throughput equation of TFRC that is somewhat a simplified version of the throughput equation for TCP-Reno [36] as it is considerably the most accepted implementation in the internet [37][38]. In addition, we model S-TFRC as performance enhancements to standard TFRC using proposed QS implementation for DCCP-TFRC.

An important thing to note that TCP-Like is similar to TCP because of the abrupt changes in the sending rate during any congestion events [2]. The TFRC, on the other hand, maintains smooth rate control between the two communicating parties [12]. In order to demonstrate this, we have implemented the S-TCPLike and have carried out extensive simulations for the performance comparison of both S-TCPLike and S-TFRC during the vertical handovers among heterogeneous wireless access technologies in one of our previous works [39]. Henceforth, here we model the behaviour of only the S-TFRC in different congestion events during the handover process.

Table 2. Description of Symbols Used in the Analytical Model

Symbols	Description
p_1	Probability of packet loss in forward direction
p_2	Probability of packet's acknowledgement receipt in the reverse direction
P_{mn}	Probability of occurrence of congestion events
T_s	Expected time duration for acknowledgment receipt
T_{mn}	Average time to remain within a congestion window
μ_1	Initial congestion window size
β	Congestion window growth rate
D_{ss}	Data segments transmitted in unconstrained event in the slow-start
P_{eds}	Expected number of data segments successfully sent during slow-start
T_{TFRC}	TFRC sender rate calculated though TCP throughput formula [2]
W_{ss}	Expected data segments sent at the end of slow-start
ET	Expected time at the end of slow-start
P_{TO}	Probability of timeout
T_{TO}	Timeout duration

Our objective from this analytical model is to quantify the effect of handovers on rate control, based on closed form of TCP throughput equation, which is entirely a different congestion control mechanism and is based on loss event rate and sustained average RTT . For simplicity of the model we assume that the TFRC is implemented in one direction. For this, we define p_1 as the probability of packet loss in forward direction and p_2 as the probability of packets' acknowledgement receipt in the reverse direction with the RTT being the average round trip time between the two end nodes. Complete set of symbols used in analytical model is given in Table 2. Let P_{mn} be the probability that the sending congestion window successfully moves after it experiences exactly m failures for transmitting data segments and its successful transmission. Followed by exactly n failures of transmitting ACKs and then successful ACK received, as:

$$P_{mn} = p_1^m (1 - p_1) \cdot p_2^n (1 - p_2) \quad (1)$$

During this process, if the sender does not receive ACK intended for a specific data segment after some time duration T_s (initially three seconds [40] and waits twice as long for a response) then it retransmits the data segment after a timeout, which is set to $4RTT$ [2]. The time it takes for this whole process is T_{mn} .

$$T_{mn} = 4RTT + \sum_{i=0}^{m-1} 2^i T_s + \sum_{i=0}^{n-1} 2^i T_s \quad (2)$$

To smoothly maintain the TFRC sending rate; the congestion window under the TFRC moves if at least half of the packets are acknowledged [2]. We calculate it as the expected number of data segments transferred and each round the sender receives at least $cwnd/2$ ACKs. Since the sender rate depends upon how much data segments are successfully received at the receiver [2]. Let $cwnd_i$ be the sender congestion window at the beginning (round i) so congestion window during the next round can be calculated as $cwnd_{i+1} = cwnd_i + cwnd_i/b$ which corresponds to $\beta cwnd_i$. Here b is the number of packets acknowledged by a single TCP acknowledgment [2]. The sender TFRC in the

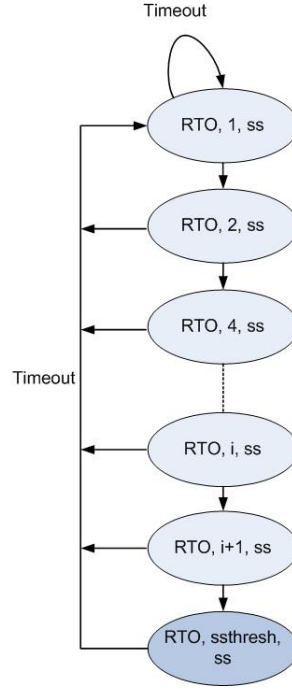


Fig. 5. TFRC Sending rate behavior in absence of loss rate.

absence of any loss event, such as timeout, remains in the same state or enters the congestion avoidance phase if it crosses the threshold. The sending window behavior for this process is shown in Figure 5.

Let μ_1 be the initial congestion window size that is used for transmission at the start then the congestion window can be approximated as a geometric series ($D_{ss} = \mu_1 + \mu_1 \cdot \beta + \mu_1 \cdot \beta^2 + \dots + \mu_1 \cdot \beta^{i-1} = \mu_1 \cdot (\beta^i - 1) / (\beta - 1)$) for each subsequent rounds. Thus D_{ss} is the number of data segments that are successfully sent each time before any congestion event occurs conditioned to when the loss event rate becomes greater than 0 (i.e. $P_{mn} > 0$). We refer the term D_{ss} as d that are the data segments transmitted in an unconstrained event in the slow-start (since the $P_{mn} = 0$, which means that if there is no loss then the sender is in the slow-start ss [2]). This phase of the data transmission keeps increasing until either of three transitions occur during the data transmission i.e. sender observes the loss event rate due to data segment loss, or the sender does not receive ACK due to timeout, or the feedback timer expires [2]. These three congestion events along with their impact on the TFRC sender rate are explained below.

6.1. Effect of loss Event Rate due to Data Segment loss

In the absence of any loss event, the sender remains within the slow-start phase and each RTT it doubles its sending rate. Let P_{eds} be the probability of expected number of data segments sent and can be calculated as:

$$P_{eds} = (1 - P_{mn}) \cdot d \quad (3)$$

When all the data segments are successfully sent and their corresponding ACKs are correctly received i.e. $P_{mn} = 0$ (i.e.) then above equation can be re-written as $P_{eds} = d$. Hence all the data segments d are sent successfully in an unconstrained event. On the other hand, $P_{mn} > 0$ (some of the data packets are not acknowledged or ACK packets are lost) then P_{eds} can be calculated after at least half of the data segments Dss are not acknowledged in each round:

$$P_{eds} = \sum_{\mu_1=0}^{d-1} (1 - P_{mn})^{\mu_i} \cdot P_{mn} \cdot \mu_i \quad (4)$$

Depending upon P_{eds} , we calculate the sender TFRC rate according to TCP's throughput equation and the corresponding RTT is updated. We assume that the sender TFRC knows its current sending rate (X), maintains recent value of round trip time (R) and an estimate of the updated timeout interval since the last event occurred. In view of the fact that new sending rate is calculated every time it receives a feedback packet; we assume that because of the absence of any loss event rate the feedback packet has no effect over the sending TFRC rate. Hence, the sender doubles its sending rate (i.e. $2 \cdot X_{recv}$ (received sender rate)) each round. However, a new rate is calculated after a loss event rate is reported (for $P_{mn} > 0$), in which case the sender rate is calculated as follows:

$$X = \max(\min(T_{TFRC}, 2 \cdot P_{eds} \cdot (1 - P_{mn})), s/64) \quad (5)$$

Here the term T_{TFRC} refers to the TCP throughput equation to regulate sender's rate, s is the packet size in bytes, 64 is the time in seconds referring to maximum inter-packet backoff interval in the continuous absence of feedback packets. This means that the sender sends at least one packet every 64 seconds when $P_{mn} > 0$. On the other hand, if $P_{mn} = 0$ in above equation then the sending rate is doubled each time the sender rate is calculated. The corresponding RTT is updated as [2] $R = q \cdot R + (1 - q) \cdot R$.

The sender TFRC rate in terms of expected number of data segments sent each round ($i = \log_{\beta} (Dss(\beta - 1)/\mu_1 + 1)$ termed as total rounds before any event occurs) without any loss event rate can be calculated as $Wss = \mu_i \cdot i = \mu_i \cdot (Dss(\beta - 1)/\mu_1) \cdot \beta^{-1}$. The expected time it takes a sender to send the data segments in an unrestricted slow start or after a loss event occurs, can be calculated as:

$$ET = RTT \cdot (Wss + P_{eds}) \quad (6)$$

6.2. Effect of Timeout

The probability of timeout is to happen when a packet is not acknowledged for more than $3RTT$ s. The TFRC sender rate, in the case of timeout, must reflect the TCP retransmit

timeout behavior and the new rate is calculated according to TCP throughput equation [2] because it dominates the sending rate at higher loss rates. Let P'_{mn} be the probability where at least m number of data packets are not acknowledged, the timeout probability is given as:

$$P_{TO} = P'_{mn} = \sum_{(m,n)=1}^4 P_2^n \cdot (1 - P_1)^m \quad (7)$$

The TFRC sending rate depends on the duration of timeout and the subsequent number of timeouts that occur. The time it takes after which the timeout can occur is given as:

$$T_{TO} = \sum_{i=1}^4 RTT_i \cdot P_{TO} \quad (8)$$

The TFRC sending rate, by first calculating the TCP throughput after timeout occurs, can be calculated as [2]:

$$T_{TFRC} = s / (R\sqrt{2 \cdot b \cdot p/3}) + (T_{TO} \cdot (3 \cdot \sqrt{3 \cdot b \cdot p/8} \cdot p \cdot (1 + 32 \cdot p^2))) \quad (9)$$

Here s is the packet size, T_{TO} is the calculated timeout, p is the corresponding loss event rate, b are the number of packets acknowledged by a single TCP acknowledgment, and R is the calculated round trip time.

6.3. Effect of no-Feedback Timer Expiration

The feedback from the receiver is sent every RTT and contains the following information: the calculated loss event rate as estimated by the receiver, time stamps used by sender to estimate the round trip times, and the previous rate received at the receiver. The feedback timer is set to at least $4RTT$ s and each time if the sender does not receive feedback from the receiver then the sending rate is cut to half.

The authors in [41] presented an estimation of the probability of detection of packet loss as a result of expiration of $4RTT$ s. We use the same estimation as in [41] for the probability when the feedback timer expires. This is given as:

$$Q(p, w) = \min \left(1, \frac{(1 - (1 - p)^3)(1 + (1 - p)^3(1 - (1 - p)^{w-3}))}{1 - (1 - p)^n} \right) \quad (10)$$

The expected cost in terms of latency of the retransmit timeout is calculated as:

$$E[Z^{TO}] = RTO \cdot \frac{1 + p + 2p^2 + 4p^3 + 8p^4 + 16p^5 + 32p^6}{(1 - p)} \quad (11)$$

The exponential growth of the subsequent consecutive j no-feedback timer expiration is:

$$L_h = \begin{cases} (2^j - 1) RTO & j < 6 \\ (63 + 64(j - 6)) RTO & j \geq 7 \end{cases} \quad (12)$$

Each time the sender receives a feedback packet; the sender TFRC sets the no-feedback timer to expire after $\max(4R, 2s/X)$ [2].

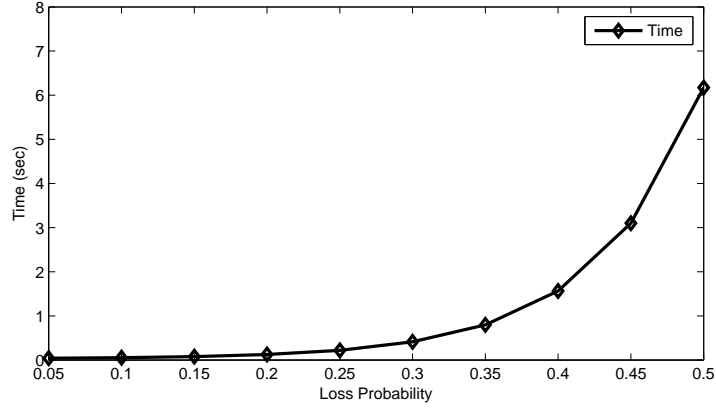


Fig. 6. Average Time to remain within a particular Congestion Window and frequency of Loss Distribution.

6.4. S-TFRC Modeling

We now present the S-TFRC implementation based on Quick-Start proposed for DCCP [31]. It enables the sender TFRC to cooperate with the intermediate nodes (e.g. routers) along with the end subscribers to agree over maximum possible sending rate for an ongoing session during vertical handovers.

S-TFRC sender may initiate QS process during the start of connection establishment to start with larger initial rate or during the connected S-TFRC flows when $P_{mn} > 0$ due to some congestion events or after an idle time period. To model the process of proposed QS implementation, we represent initial QS interval to QSI . This value is set to sufficiently large time to prevent intermediate router process over typical internet paths [31]. This becomes more important when we consider various heterogeneous technologies with diverse link characteristics and various mobility distributions and link stabilities.

The subsequent QS request intervals are scheduled to $\max(QSI \cdot 2, 4 \cdot RTT)$ and are doubled after each unsuccessful QS requests. This can backoff to a maximum of 64 seconds [31] so that the end nodes could find sufficient time to prevent unnecessary processing in resulting the QS approval. The feedback timer is set at the start and end of the periods in which QS packets are sent that results in feedback to be sent to the sender TFRC. The sender on receipt of the QS response does not enter into QS mode if QS rate is less than the current sending rate (X) or any congestion or loss events are reported. The sending S-TFRC, however, enters QS mode at the time when approved QS rate (QXR) exceeds X and continues over newly calculated rate. The QS exists when a period of $1RTT$ is passed, or any congestion or loss event is detected or a feedback packet is received that acknowledges one or more QS packets. The QXR is calculated as [31]:

$$QXR = (QSR \cdot s) / (s + H) \quad (13)$$

Where QSR is the rate request approved during the QS process, s is the packet size and H is the TFRC/IP header.

7. Validation of Analytical Model

In this section, we validate our analytical model for various vertical handovers and link stabilities via simulations. For analytical model evaluation, we consider large file transfer for a duration of 10,000sec. We also take an average RTT of 100ms, segment size ranging from 512-1000bytes, an initial window size of 1, and slow-start threshold of 32, 64, 128, or 256 with no link losses. Finally we take the loss rates with $p1 = 0.0$ and $0.0 \leq p2 \leq 1.0$ and then $p2 = 0.0$ with $0.0 \leq p1 \leq 1.0$ to simulate diverse loss probabilities in forward and reverse directions. Figure 6 shows the time it takes to recover from congestion events or increase in loss rate. This figure shows that when probability of P_{mn} increases, the time to renegotiate and resume the established connection during the handover process also increases. Hence, we first want to evaluate the congestion behavior of various transport layer protocols by evaluating the change in congestion window under different mobility distributions and then give its impact over the handover process in Section 8.

Figure 7 (a) and (b) shows the sending rate behavior as the number of packet sent each RTT using TCP, standard TFRC, and proposed S-TFRC using both simulation and analytical model evaluations (solid lines in Figure 7 (a) and (b)). It can be observed that the congestion window behavior for various RTT s, using both the analytical model and simulations results show similar behavior for TCP and S-TFRC. The average number of packets sent every RTT using analytical model and simulations for S-TFRC is $20pkts/RTT$ and $18pkts/RTT$, respectively. It can be observed that $pkts/RTT$ for analytical model are little higher as compared to that of simulations. The reason for this is that the analytical model does not estimate exact delays at queues, links and routers processing.

Another important observation from these evaluations is that the S-TFRC performs better than the TFRC. For instance, at 14th RTT , only $12pkts/RTT$ packets are sent with TFRC while with S-TFRC approximately $20pkts/RTT$ packets are sent. Our simulation and analytical results for Pareto (not shown in Figure 7 and is discussed later in Section 8) and Exponential distributions also show that S-TFRC performs better than the standard TFRC. Furthermore, our analysis reveals that S-TFRC performs better for U-distribution ($20pkts/RTT$) followed by P-distribution ($19pkts/RTT$) and then followed by the E-distribution ($17pkts/RTT$). For E-distribution, we note that the end S-TFRC nodes do not find sufficient time to adjust their improved rates and the probability of going through the QS mode becomes less.

8. Results & Discussion

In the last Section 7, we validated the performance of proposed model using extensive simulations. Now in this section, we further study the behavior of S-TFRC as compared to standard TFRC with results obtained from simulations and analytical model. We first present some analytical results to study the performance gain achieved with S-TFRC as compared to standard TFRC during vertical handovers among heterogeneous technologies with different link stabilities and mobility distributions. Figure 8 compares sender transmission rate ($pkts/RTT$) for standard TFRC and S-TFRC in U, E, and P distributions and various link stabilities. As shown in Figure 8, S-TFRC performs better than the standard TFRC for all distributions. For example, the S-TFRC achieves an average sender rate of $31pkts/RTT$, $28pkts/RTT$, and $25pkts/RTT$ as compared to TFRC

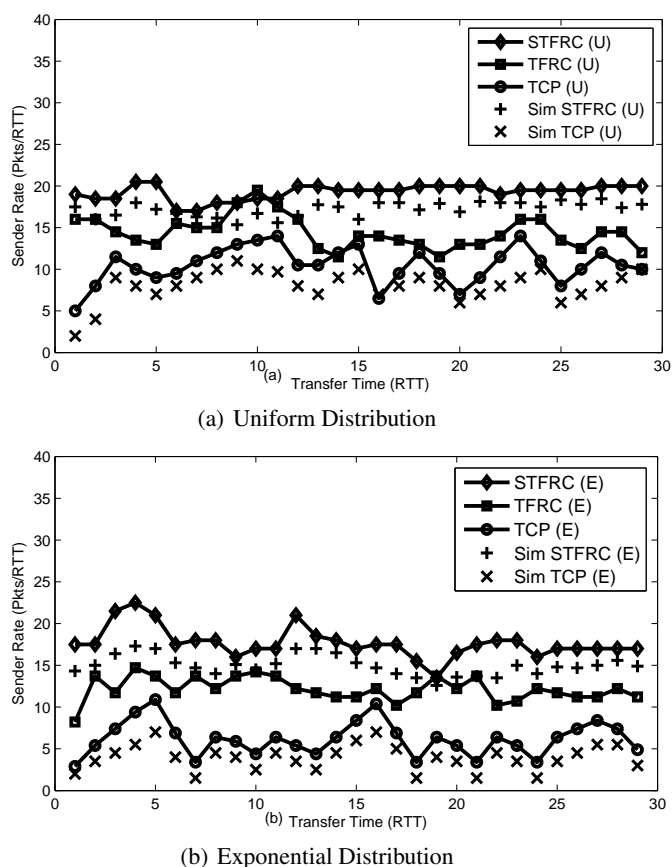


Fig. 7. Congestion Window behavior from Simulation and Analytical Model with S-TFRC, TFRC, and TCP (a) Uniform Distribution (b) Exponential Distribution.

with $25\text{pkts}/RTT$, $23\text{pkts}/RTT$, and $19\text{pkts}/RTT$ respectively for each of the U, E, and P distributions.

Figure 9 shows a plot depicting the average throughput obtained in the presence of loss rates as experienced by standard TFRC (U) and S-TFRC (U) using analytical model. It has observed that initially both the flows experience no losses and achieve good throughput, but the average throughput of both TFRC and S-TFRC degrades as loss rate increases. However, S-TFRC still achieves higher throughput at each of the different loss rates. As an example, at the loss rate of 0.1%, S-TFRC achieves an average throughput of 7.85kbps while TFRC achieves an average throughput 6.58kbps. We observe that S-TFRC performs better and achieves 19.57% improved throughput as compared to TFRC.

We now present, via simulations, the performance of the proposed S-TFRC in terms of transmission delays, throughput, transmission rates and transmission losses for real time multimedia applications during vertical handovers. We calculate delay as the time duration when transport layer waits for handover process to complete, and resumes end-

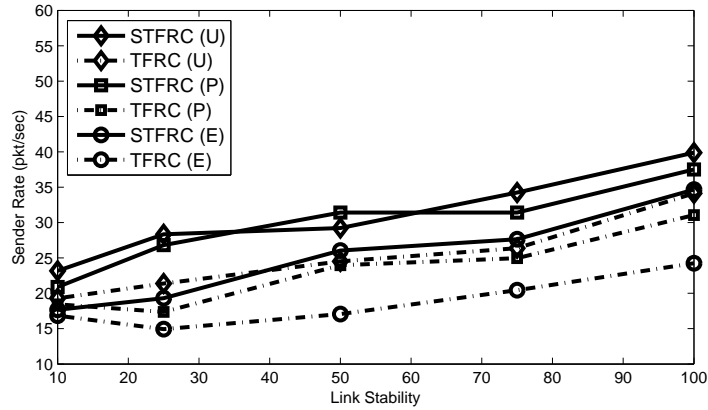


Fig. 8. Sender Rate for S-TFRC and TFRC in various Handover Distributions via Analytical Model.

Table 3. Performance Comparison of S-TFRC and TFRC

Parameters	Uniform		Exponential		Pareto	
	TFRC	S-TFRC	TFRC	S-TFRC	TFRC	S-TFRC
Average Transmission Delay (ms)	16.4	13.4	100	38.9	19.9	13.2
Average Sender Rate *10 ⁻⁵ (bps)	1.0	2.4	0.09	0.15	0.25	1.5
Average Throughput (Mbps)	0.59	0.7	0.01	0.012	0.06	0.17

to-end data transport. The actual value, however, comprises of delay caused at physical, data link, and network layers where Mobile IP provides the necessary binding between the MN, foreign agent (FA) and HA. The maximum time for this to complete is set as $(2 * RTT + 100ms)$ [10]. However, our calculation only focuses on delays at the transport layer corresponding to timeout, no-feedback timer, round trip times, etc., which for standard TFRC is a result of slow start and congestion avoidance while for S-TFRC it is the time that S-Feedback responds with new transmission rate. For example, when MN handovers to WiMAX this max time is 160ms. This value is taken out from our transmission delay calculations for handover to WiMAX.

Figure 10 (a) and Figure 10 (b) compares, respectively, the transmission delay and transmission loss behaviors for standard TFRC and S-TFRC with respect to handover delays and loss distributions. We consider a near ideal link and take transmission losses as 0.02% - 0.07%. It is observed that for poor frequency of handovers; TFRC stabilizes and results in lower retransmission delays. However, with lower link stabilities; the mobile subscribers re-register the new access links with higher delays making the previous link and receiver states unusable. Furthermore, this creates misunderstanding between the respective nodes, if higher loss events are reported where the sender cannot distinguish between handovers, packet errors and congestions, therefore presumes the network as cloggy. This further hinders resuming of normal transmission and observe greater delays

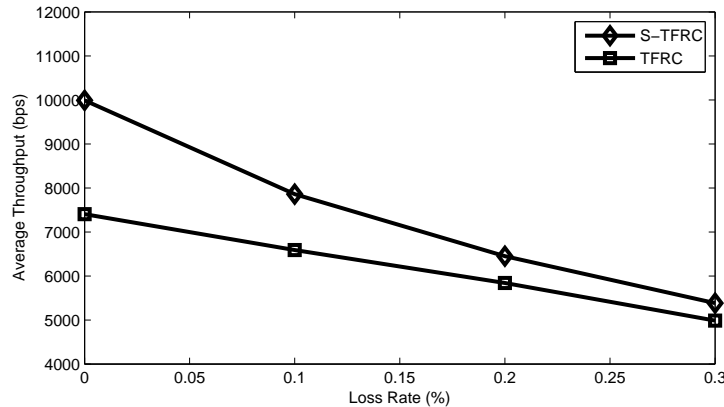
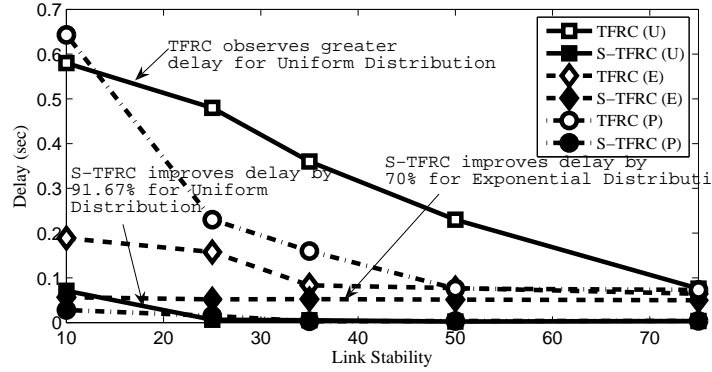


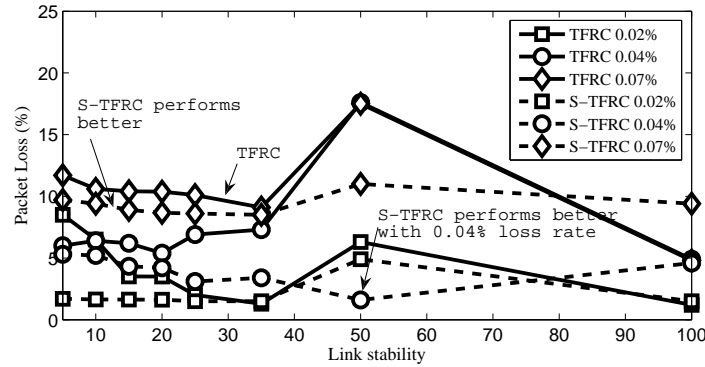
Fig. 9. Average Throughput (Mbps) obtained for S-TFRC and TFRC via Analytical Model.

to resume subsequent transmissions. However, S-TFRC timely negotiates link changes, successfully determines new transmission parameters with S-Request/S-Response rather than several RTTs. As a result, it minimizes queuing delays. As an example, in Figure 10 (a), a highly unstable link with minimum losses causes an average delay of 0.6ms for U-TFRC while for S-TFRC an average delay as low as 0.05ms is observed, performing 91.67% efficiently. Similarly, for P handovers with S-TFRC, reduces transmission delay by almost 64.47% at link stability of 35. For Exponential handovers S-TFRC provides an improvement of 70%. For U and E-handovers, S-TFRC performs better because the system tends to predictability; frequency and occurrence of handovers becomes deterministic. Similarly, in Figure 10 (b) with the worst packet loss rate of 0.07%, less packet loss is observed for S-TFRC than for TFRC e.g. at link stability of 50, the packet loss with S-TFRC is 10% while for TFRC this packet loss is 18%.

Figure 11 (a) and Figure 11 (b) compares sender transmission rate and throughput for standard TFRC and S-TFRC in U, E, and P distributions of handovers. For U-handovers, the system becomes predictable and the corresponding hosts understand the behavior of link change and therefore adjust smoothly. S-TFRC improves transmission rate by almost 1.47% compared to standard TFRC. Similar observations are also observed for throughput. For instance, for U-handovers, S-TFRC gives an average throughput of 0.4Mbps compared to 0.15Mbps for standard TFRC when link stability is 25; the 'dashed line with squares pointers' in Figure 11 (b) shows throughput for standard TFRC and 'solid line with squares pointers' in Figure 11 (b) shows throughput for S-TFRC. Similar improvements in throughput are also provided by S-TFRC for P-handovers. Table 3 summarizes the entire discussion. It clearly shows that the proposed S-TFRC works for all distributions and greatly improves performance over standard TFRC for multimedia sessions in a wireless heterogeneous system.



(a) Transmission Delay



(b) Transmission Loss

Fig. 10. Transmission Delay and Transmission Loss behaviors of S-TFRC and TFRC in various Handover Distributions via Simulation Model.

9. Conclusion

Integration of future wireless technologies with the legacy communication systems is recently becoming an important trend in wireless networking. In this paper we have introduced the concept of using link information for a better handoff. Specifically, we have proposed S-TFRC as a mechanized feedback scheme that gathers context i.e. handover and link information, which timely negotiates transport mechanisms and decides on transmission parameters after handover. We proposed a Markov model that illustrates S-TFRC protocol behavior in various congestion events of timeouts, loss rates, and no-feedback timer expiration that may happen during vertical handover process. We have validated our proposed analytical model through simulations and also found that S-TFRC greatly assists multimedia transport and reduces transmission delay after handover compared to the standard TFRC. Our results show that the S-TFRC does not penalize applications during the handover events as seen from its better transmission rate and improved throughput irrespective of the user's mobility. We conclude from our results that during vertical han-

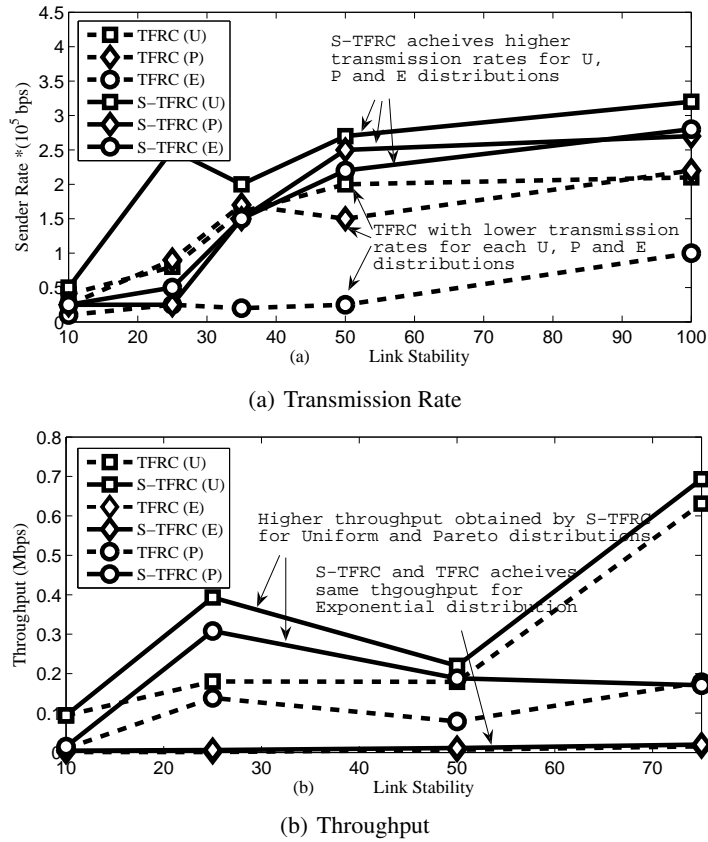


Fig. 11. Transmission Rate and Throughput for S-TFRC and TFRC in various Handover Distributions via Simulation Model.

doers our proposed S-TFRC that is assumed to have support from network elements is capable of providing better QoS to multimedia transmissions compared to that provided by the standard TFRC. We will further evaluate, as our future work, the performance of the proposed mechanism for multiple S-TFRC flows and its co-existence with TCP flows during the vertical handover process.

References

1. Shaddad, R. Q. Mohammad, A. B. Al-Gailani, S. A. Al-hetar, A. M. and Elmagzoub, M. A. "A survey on access technologies for broadband optical and wireless networks", Journal of Network and Computer Applications, 2014.
2. Floyd, S., Kohler, E., and Padhye, J. "Profile for Datagram Congestion Control Protocol (DCCP) Congestion Control ID 3 TCP-Friendly Rate Control (TFRC)", RFC 4341, March 2006.

3. Vaughan-Nichols, S. J. "The Challenge of Wi-Fi Roaming", in *IEEE Computer Journals*, Vol. 36, No. 7, pp. 17-19, Jul 2003.
4. Perkins, C. "IP Mobility Support for IPv4", RFC 3344, Aug 2002.
5. Chakravorty, R., Vidales, P., Subramanian, K., Pratt, I. and Crowcroft, J. "Performance Issues with Vertical Handovers Experiences from GPRS Cellular and WLAN hot-spots Integration", in proceedings of IEEE Pervasive Computing and Communications Workshops (PerCom), pp. 155-164, Mar 2004.
6. Schatz, S., Eggert, L., Schmid, S., and Brunner, M. "Protocol Enhancements for Intermittently Connected Hosts", in *ACM Computer Communication Review*, Jul 2005.
7. Cerqueira, E., Janowski, L., Leszczuk, M., Papir, Z., and Romaniak, P. "Video Artifacts Assessment for Live Mobile Streaming Applications", in *Springer Journal of Future Multimedia Networking*, pp. 242-247, 2009.
8. Xu, L., and Helzer, J. "Media Streaming via TFRC An Analytical Study of the Impact of TFRC on User-Perceived Media Quality", in *Elsevier Journal on Computer Networks*, pp. 4744-4764, 2007.
9. Bhavsar, S. "WLAN-Cellular Integration for Mobile Data Networks", In *Proceedings of Communications Networks and Services Research Conference*, May 2003.
10. Korhonen, J., Park, S., Zhang, J., Hwang, C. and Sarolahti, P. "Link Characteristic Information for IP Mobility Problem Statement", Network Working Group, Internet-Draft, Jun 2006.
11. Scharf, M. "Performance Analysis of the Quick-Start TCP Extension", in *IEEE Fourth International Conference on Broadband Communications, Networks and Systems*, pp. 942-951, 2007.
12. S. Floyd, E. Kohler and J. Padhye, "Profile for Datagram Congestion Control Protocol (DCCP) Congestion Control ID 3: TCP-Friendly Rate Control (TFRC)," RFC 4342, March 2006.
13. S. Floyd, M. Handley, and E. Kohler, "Problem Statement for the Datagram Congestion Control Protocol (DCCP)," RFC 4336, March 2006.
14. J. Lai and E. Kohler, "Efficiency and Late Data Choice in a User-Kernel Interface for Congestion-Controlled Datagrams," in *Proceedings of ACM Conference on Multimedia Computing and Networking (MMCN)*, pp. 136-142, Jan. 2005.
15. D. J. Gemmell and J. Han, "Multimedia Network File Servers: Multichannel Delay-Sensitive Data Retrieval," *Multimedia System*, 1(6):240-252, 1994.
16. C. M. Aras, J. F. Kurose, D. S. Reeves, and H. Schulzrinne, "Real-Time Communication in Packet-Switched Networks," in *Proceedings of the IEEE*, vol. 82 No. 1, pp. 122-139, Jan 1994.
17. Matinkhah, S. M., Khorsandi, S., Yarahmadian, S. "A new Handoff Management System for Heterogeneous Wireless Access Networks", in *International Journal of Communication Systems*, 2012.
18. Omheni, N and Zarai, F and Obaidat, MS and Hsiao, K-F and Kamoun, L. "A Novel Media Independent Handover-Based Approach for Vertical Handover over Heterogeneous Wireless Networks", in *International Journal of Communication Systems*, 2013.
19. Shahriar, Abu Zafar M and Atiquzzaman, Mohammed and Ivancic, William. "Network Mobility in Satellite Networks: Architecture and the Protocol", in *International Journal of Communication Systems*, 2011.
20. Chen, Yuh-Shyan and Hsu, Chih-Shun and Cheng, Ching-Hsueh. "Network Mobility Protocol for Vehicular ad hoc Networks", in *International Journal of Communication Systems*, 2013.
21. Salih, Yass K and Hang See, Ong and Ibrahim, Rabha W and Yussof, Salman and Iqbal, Azlan. "A Novel Noncooperative Game Competing Model Using Generalized Simple Additive Weighting Method To Perform Network Selection In Heterogeneous Wireless Networks", in *International Journal of Communication Systems*, 2014.
22. Yang, Shun-Fang and Wu, Jung-Shyr and Hwang, Bor-Jiunn. "Performance Evaluation of Priority Based Adaptive Multiguard Channel Call Admission Control For Multiclass Services in Mobile Networks", in *International Journal of Communication Systems*, 2011.

23. Qiu, Feng and Luo, Hongbin and Li, Xiaoqian and Xue, Miao and Dong, Ping and Zhang, Hongke. "A Mapping Forwarding Approach for Supporting Mobility in Networks With Identifier/Locator Separation", in *International Journal of Communication Systems*, 2011.
24. Tawil, R., Guy P., and Jacques D.. "Distributed handoff decision scheme using MIH function for the fourth generation wireless networks." , in *IEEE 3rd International Conference on Information and Communication Technologies (ICTTA): From Theory to Applications*, pp. 1-6, 2008.
25. Savitha K, Chandrasekar C. "Vertical handover decision schemes using SAW and WPM for network selection in heterogeneous wireless networks", in *Global Journal of Computer Science and Technology*; 11(9):1924, 2011.
26. Savitha K, Chandrasekar C. "Trusted network selection using SAW and TOPSIS algorithms for heterogeneous wireless networks", in *International Journal of Computer Applications*; 26(8):2229, 2011.
27. Savitha K, Chandrasekar D. "Network selection using TOPSIS in vertical handover decision schemes for heterogeneous wireless networks", in *International Journal of Computer Science (IJCSI)*; 8(3):400406, 2011.
28. Smaoui I, Zarai F, Bouallegue R, Kamoun L. "Multi-criteria dynamic access selection in heterogeneous wireless networks", in *6th International Symposium on Wireless Communication Systems 2009*; 338342.
29. Savitha K, Chandrasekar D. "Grey relation analysis for vertical handover decision schemes in heterogeneous wireless networks", in *European Journal of Scientific Research*; 54(4):560568, 2011.
30. Wang L, Binet D. "MADM-based network selection in heterogeneous wireless networks: A simulation study", in *1st International Conference on Wireless Communication, Vehicular Technology, Information Theory and Aerospace & Electronic Systems Technology 2009*; 559564.
31. Fairhurst G., and Sathiseelan, A. "Quick-Start for Datagram Congestion Control Protocol (DCCP)", DCCP Working Group IETF, Internet-Draft, June 2009.
32. Zhang, J., Korhonen, J., Park, S., and Pearce, D. "TCP Quick-Adjust by Utilizing Explicit Link Characteristic Information", in *International Workshop on Performance Analysis and Enhancement of Wireless Networks (PAEWN)*, 2008.
33. Gurtov, A., and Korhonen, J. "Effect of Vertical Handovers on Performance of TCP-Friendly Rate Control", in *ACM Mobile Computing and Communications Review*, Vol. 8, No. 3, pp. 73-87, 2004.
34. Gao, W., Faulkner, J. "Performance Evaluation of a Cognitive Radio Network with Exponential and Truncated Usage Models", in *IEEE International Symposium on Wireless Pervasive Computing*, 2009.
35. Musa, A. Angappa G. Yahaya Y. and Abdelrahman A. "Embedded devices for supply chain applications: Towards hardware integration of disparate technologies." *Expert Systems with Applications* 41, no. 1, 137-155, 2014.
36. Padhye, J., Firoiu, V., Towsley, D., and Kurose, J. "Modeling TCP Throughput A Simple Model and its Empirical Validation", *ACM Special Interest Group on Data Communication (SIGCOM) Computer Communication Review*, vol. 28, no.4, pp. 303-314, 1998.
37. Paxson, V. "Automated Packet Trace Analysis of TCP Implementations", *ACM SIGCOMM conference on Applications, Technologies, Architectures, and Protocols for Computer Communication*, pp. 167-179, 1997.
38. Paxson, V. "End-to-End Internet Packet Dynamics", *ACM Special Interest Group on Data Communication (SIGCOM) Computer Communication Review*, vol. 27, no. 4, pp.139-152, 1997.
39. Shah, Z. Baig, A. Samir, H. and Ullah, I. "State Aware Enhancement in DCCP for Multimedia Handovers", In the *IEEE Proceedings of Global Communications Conference (Globecom)*, Anaheim, California, US, Dec 2012.

40. Braden, R. "Requirements for Internet Hosts - Communication Layers", RFC 1122, October 1989.
41. Stevens, R. "TCP/IP Illustrated", vol. 1, Addison-Wesley New York, 1994.

Imdad Ullah received his MS.IT from School of Electrical Engineering and Computer Science (SEECS), National University of Sciences & Technology (NUST), Islamabad, Pakistan. He is currently a PhD candidate at The University of New South Wales (UNSW), Sydney, Australia. His current research interests include Wireless Communications, Wireless Mesh Networks, Network Modelling and Design, Optimization Theory, Trusted Networking, and Privacy.

Zawar Shah received the Bachelors of Computer Engineering from National University of Sciences & Technology (NUST), Islamabad, Pakistan in 2003. He completed his M.EngSc and PhD degree in Telecommunications from the University of New South Wales (UNSW), Sydney, Australia in 2004 and 2009, respectively. He was the head of the Telecommunications department at the School of Electrical Engineering and Computer Science (SEECS), which is a constituent college of NUST, Pakistan. He is currently working as a Senior Lecturer at Whitireia Community Polytechnic, Auckland, New Zealand. His research interests include QoS issues in Wireless Networks, Vertical Handover issues between 3G/4G networks, Cloud Computing, Network Architectures and Protocols.

Adeel Baig received the B.E. from the NED University of Engineering and Technology, Karachi, Pakistan, and the M.Eng.Sc. and Ph.D degree in Computer Science and Engineering from the University of New South Wales (UNSW), Australia. He is an Assistant Professor at the College of Computer and Information Systems, Al Yamamah University, Saudi Arabia. He is also affiliated with the School of Electrical Engineering and Computer Science at the National University of Sciences & Technology (NUST) Pakistan, where he co-directs the Center of Excellence in IP Technologies. Before joining NUST, he held several positions in research and teaching, including with National ICT Australia (NICTA) and with UNSW. His research interests include cognitive and mobile networks, cross layer optimization for wireless networks and IPv6 deployments and transition issues. Dr. Baig has been a member of technical program committees of several local/international conferences. He is also a member of the IEEE, ACM, PEC and ISOC.

Received: January 22, 2015; Accepted: August 8, 2015.

